HHS Public Access

Author manuscript

Virology. Author manuscript; available in PMC 2022 October 19.

Published in final edited form as:

Virology. 2020 September ; 548: 49–58. doi:10.1016/j.virol.2020.06.006.

Identification of a Novel Signaling Complex Containing Host Chemokine Receptor CXCR4, Interleukin-10 Receptor, and Human Cytomegalovirus US27

Carolyn C. Tu[1], **Christine M. O'Connor**[2], **Juliet V. Spencer**[1,3]

[1]Department of Biology, University of San Francisco, San Francisco, CA 94117 USA

[2]Genomic Medicine, Lerner Research Institute, Cleveland Clinic, Cleveland, OH 44195 USA

[3]Department of Biology, Texas Woman's University, Denton, TX 76204 USA

Abstract

Human cytomegalovirus (HCMV) is a widespread herpesvirus that establishes latency in myeloid cells and persists by manipulating immune signaling. Chemokine receptor CXCR4 and its ligand CXCL12 regulate movement of myeloid progenitors into bone marrow and out into peripheral tissues. HCMV amplifies CXCL12-CXCR4 signaling through viral chemokine receptor US27 and cmvIL-10, a viral cytokine that binds the cellular IL-10 receptor (IL-10R), but precisely how these viral proteins influence CXCR4 is unknown. We used the proximity ligation assay (PLA) to examine association of CXCR4, IL-10R, and US27 in both transfected and HCMV-infected cells. CXCR4 and IL-10R colocalized to discrete clusters, and treatment with CXCL12 and cmvIL-10 dramatically increased receptor clustering and calcium flux. US27 was associated with CXCR4 and IL-10R in PLA clusters and further enhanced cluster formation and calcium signaling. These results indicate that CXCR4, IL-10R, and US27 form a novel virus-host signaling complex that enhances CXCL12 signaling during HCMV infection.

Graphical Abstract

Corresponding Author: Juliet Spencer, Texas Woman's University, 301 Research Circle, GRB 201, Denton, TX 76205, +1-940-898-2352, JSpencer7@twu.edu.

Credit Author Statement:

Carolyn C. Tu: Conceptualization, Methodology, Formal analysis, Investigation, Writing – Original draft preparation, Visualization.
Christine O'Connor: Resources, Writing – Reviewing and Editing.
Juliet V. Spencer: Conceptualization, Formal analysis, Writing – Reviewing and Editing, Visualization, Supervision, Funding Acquisition.

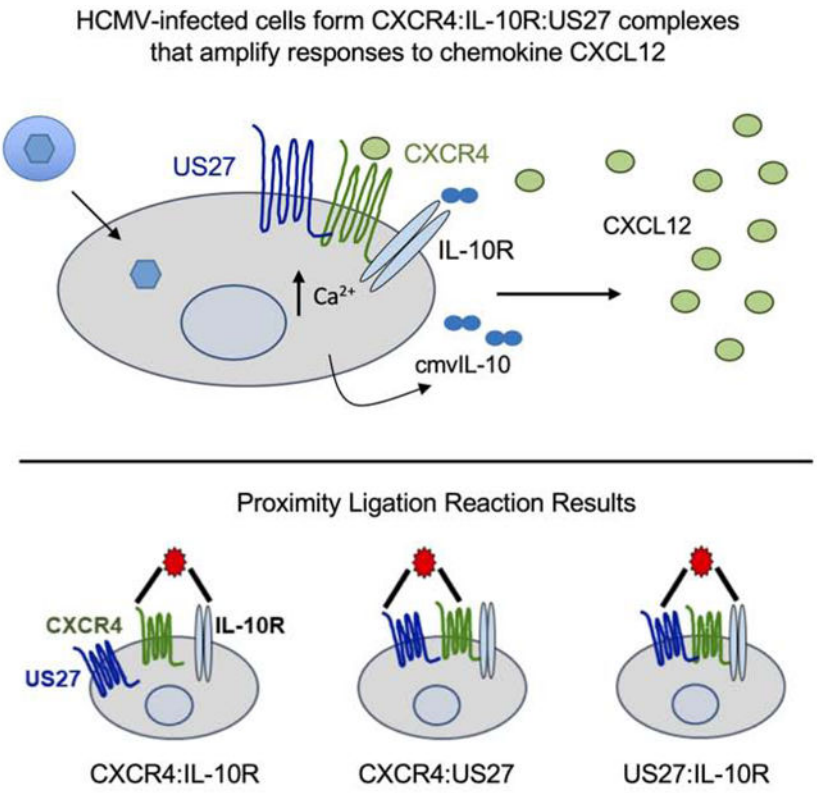

Keywords

Chemokine; cmvIL-10; CXCL12; CXCR4; cytokine; cytomegalovirus; HCMV; interleukin-10; IL-10R; proximity ligation assay; US27

Introduction

Human cytomegalovirus (HCMV) is a member of the *Herpesviridae* family and a widespread pathogen that can establish lifelong latent infection (Jackson et al., 2011; Mocarski, 2006). Worldwide seroprevalence ranges from 70–90% in the general population and infection is usually asymptomatic or mild and flu-like in healthy individuals (Cannon et al., 2010). HCMV infection can be life-threatening in immune-compromised hosts, and transplant recipients and AIDS patients are prone to reactivation of latent virus, resulting in serious conditions like retinitis and pneumonitis (Azevedo et al., 2015; Soderberg-Naucler, 2008). HCMV is the most common viral cause of birth defects and childhood disabilities in the United States (Cannon, 2009). While a vaccine is considered a high priority (Arvin et al., 2004), development has been challenging due to extensive manipulation of immune responses by HCMV.

The HCMV UL111A gene encodes cmvIL-10, a viral ortholog of human interleukin-10 (hIL-10) (Kotenko et al., 2000). Despite having only 27% amino acid sequence identity to hIL-10, cmvIL-10 exhibits the same immunosuppressive properties as hIL-10, such as inhibition of pro-inflammatory cytokines and down-regulation of major histocompatibility

complex (MHC) expression (Slobedman et al., 2009; Spencer et al., 2002). CmvIL-10 binds and signals through the hIL-10 receptor (IL-10R) (Kotenko et al., 2000). Upon engagement by either hIL-10 or cmvIL-10, the IL-10R dimerizes and activates Janus kinases JAK1 and Tyk2, which phosphorylate and activate STAT3 (signal transducer and activator of transcription 3). STAT3 dimerizes and translocates to the nucleus to activate expression of target genes. CmvIL-10 is produced during both lytic and latent infection and has the ability to broadly impact host immune function.

In contrast to the potent immune suppressive effects reported for cmvIL-10, we found that cmvIL-10 significantly heightens signaling responses through CXCR4 (C-X-C Motif Chemokine Receptor 4) (Tu et al., 2018). CXCR4 is a member of the G protein-coupled receptor (GPCR) superfamily and regulates cell movement during development, hematopoiesis, tumor metastasis, and immune responses. The natural ligand for CXCR4 is chemokine CXCL12, also known as SDF-1α (stromal derived factor-1 alpha), which is highly expressed in stromal tissues. Engagement of CXCR4 by CXCL12 induces conformational changes that lead to G protein activation, calcium release, and chemotaxis along the chemokine gradient. CmvIL-10 binding to the IL-10R caused increased calcium flux and chemotaxis in response to CXCL12 (Tu et al., 2018). Balabanian et al. found that hIL-10 potentiated the proliferative and chemotactic effects of CXCL12 on B lymphocytes, while other cytokines such as IL-5, IL-6, and IL-9 had no effect (Balabanian et al., 2002). Taken together, these findings indicate crosstalk between IL-10R and CXCR4 and suggest that HCMV could alter CXCR4 signaling outcomes with cmvIL-10 during infection.

CXCR4 is a highly tunable receptor and its signaling can be altered through interactions with other receptors, most notably chemokine receptors CCR2 and CXCR7, which dampen responses to CXCL12 (Levoye et al., 2009; Sohy et al., 2007). HCMV encodes four chemokine-like GPCRs: US27, US28, UL33, and UL78 and all modulate CXCR4 signaling. US28, UL33, and UL78 impair various CXCR4 functions (Frank et al., 2016; Tadagaki et al., 2012), while US27 enhances CXCL12-CXCR4 signaling outcomes (Arnolds et al., 2013; Tu et al., 2018).

Of the four HCMV GPCRs, US27 is expressed during lytic infection only (Humby and O'Connor, 2015). US28, UL33, and UL78 are expressed during both lytic and latent infection (Beisser et al., 2001; Cheng et al., 2017). US28 binds and signals in response to multiple host chemokines (Krishna et al., 2018). In contrast, US27, UL33, and UL78 are orphan receptors with no known response to chemokines (Arnolds et al., 2013; Bodaghi et al., 1998). However, US27, US28, and UL33 exhibit constitutive, ligand-independent signaling (Boeck et al., 2018; Casarosa et al., 2001; Casarosa et al., 2003). All four receptors are part of HCMV virions (Fraile-Ramos et al., 2001; Fraile-Ramos et al., 2002; Humby and O'Connor, 2015; Margulies et al., 1996; Margulies and Gibson, 2007; Varnum et al., 2004), suggesting that when virus fuses with the cell membrane, these viral GPCRs (vGPCRs) could immediately influence cell-signaling networks and cell-trafficking patterns.

Using the proximity ligation assay (PLA), we previously reported that CXCR4 was closely associated with US27 in membranes of infected cells (Tu et al., 2018). PLA is a powerful technique for detecting and quantifying direct protein interactions using

complementary oligonucleotide-conjugated secondary antibodies (Soderberg et al., 2006). If the oligonucleotides are within 15–30 nm of each other, they will ligate to form a closed circle that can be amplified by rolling circle replication. The resulting concatemeric DNA can be visualized by the addition of fluorescently labeled probes that hybridize to sequences in the amplicon, forming discrete spots. In this study, we used the PLA to explore associations between CXCR4, IL-10R, and US27 in order to clarify how HCMV enhances CXCR4 signaling outcomes during infection.

Results and Discussion

CXCR4 is in close proximity to IL-10R in cell membranes

Engagement of the IL-10R amplifies signaling outcomes induced by CXCL12 binding to CXCR4 (Balabanian et al., 2002; Tu et al., 2018). We hypothesized that crosstalk between the CXCR4 and IL-10R signaling pathways required that the two receptors were in close proximity in cell membranes. The cellular distribution of endogenously expressed CXCR4 and IL-10R was examined in HEK293 cells cultured on glass coverslips. The cells were fixed, stained with antibodies directed to each receptor, and viewed by confocal microscopy. CXCR4 (green) was found on the cell surface and distributed throughout the cell (Fig 1A). IL-10R (red) exhibited a similar widespread distribution, and there was extensive overlapping of the two signals (yellow), suggesting that the two proteins colocalized to the same sites in HEK293 cells.

We also examined whether CXCR4 and IL-10R were colocalized in cells in human bone marrow, an important reservoir for HCMV latency (Sinclair, 2008). Human bone marrow tissue sections were probed with antibodies to each receptor and examined via confocal microscopy. Comparable levels of CXCR4 and IL-10R were evident, and a widespread protein distribution pattern throughout individual cells within the bone marrow was observed (Fig. 1B). In the merged image, CXCR4 and IL-10R exhibited distinct areas of colocalization (yellow). These images show CXCR4 and IL-10R are naturally expressed and colocalized in discrete sites in human bone marrow.

The PLA was employed to further investigate the association between CXCR4 and IL-10R. HEK293 cells were grown on glass-bottom chamber slides, fixed and stained with primary antibodies targeting CXCR4 and IL-10R followed by oligonucleotide-conjugated secondary antibodies. Discrete red fluorescent punctae were observed, indicating that CXCR4 and IL-10R were within 30 nm of each other in the cell (Fig. 2). To verify that the association between CXCR4 and IL-10R was specific, we evaluated proximity to another receptor that is highly expressed in HEK293 cells, the Oncostatin M receptor (OSMR). HEK293 cells stained with antibody pairs against CXCR4 and OSMR or IL-10R and OSMR did not result in any PLA spots (Fig. 2). The results confirm that CXCR4 and IL-10R are closely and specifically associated in HEK293 cell membranes.

Ligand binding increases associations between CXCR4 and IL-10R

We predicted that ligand binding might induce conformational changes that impact the association between CXCR4 and IL-10R. HEK293 cells were treated with CXCL12, then

fixed and stained with antibodies to CXCR4 and IL-10R for PLA as above. Cells treated with CXCL12 had twice as many PLA spots as untreated control cells (Fig 3A, B), indicating that ligand engagement enhances CXCR4 proximity to IL-10R. Treatment with CXCL12 + cmvIL-10 resulted in an even greater increase in the number of CXCR4:IL-10R spots, demonstrating that binding of both ligands brought even more receptors into close proximity. The increase in receptor clustering, or number of PLA spots, correlated with the intensity of downstream signaling, as measured by calcium mobilization (Fig 3C). Cells were labeled with a calcium indicator dye and stimulated with CXCL12. Binding of CXCL12 to CXCR4 induced a rapid and transient release of calcium ions that triggered peak fluorescence within seconds and rapidly tapered off. Treatment with CXCL12 + cmvIL-10 resulted in a greater level of fluorescence, or overall calcium mobilization, demonstrating that engagement of the IL-10R amplified downstream CXCR4 signaling. Treatment with cmvIL-10 alone did not induce calcium flux (Fig 3C) or enhance receptor associations (Fig 3A, B). These results show that the increase in associations between CXCR4 and IL-10R correlates with higher downstream CXCR4 signal amplitude.

HCMV US27 enhances associations between CXCR4 and IL-10R

HCMV US27 also increases CXCR4 signaling activity (Arnolds et al., 2013; Tu et al., 2018). We previously reported that US27 is in close proximity with CXCR4 in HCMV-infected cells (Tu et al., 2018), so we wondered how US27 would impact the association of CXCR4 and IL-10R. HEK293 cells stably expressing FLAG-tagged US27 or US28 were stained with antibodies targeting the FLAG epitope, CXCR4, or IL-10R. Overall expression levels between US27 and US28 were comparable throughout the cell (Fig 4). US28 exhibited a widespread distribution, while US27 had a more punctate and perinuclear localization, consistent with previous reports (Fraile-Ramos et al., 2002; Stapleton et al., 2012). IL-10R and CXCR4 exhibited colocalization with US27 as shown by yellow where the green, magenta, and red spectra overlap in merged images (Fig. 4). In contrast, US28 did not appear to colocalize with CXCR4, in agreement with previous results (Frank et al., 2016; Tu et al., 2018).

We used PLA to quantify associations between CXCR4 and IL-10R in the presence of US27. While HEK293 cells had multiple PLA spots indicating proximity of CXCR4 and IL-10R (Fig 5A), the number of spots in 293-US27 cells was greater (Fig. 5B, C). Quantification of PLA spots indicated that the presence of US27 was associated with significantly more interactions between CXCR4 and IL-10R (Fig 5B). In addition, PLA spots were observed when 293-US27 cells were stained with paired antibodies to detect US27:CXCR4 or US27:IL-10R associations (Fig 5C). Staining with paired antibodies to US27:OSMR, CXCR4:OSMR, and IL-10R:OSMR did not result in detectable PLA spots (Fig. 5C). Taken together, these results confirm that US27 is specifically associated with both CXCR4 and IL-10R and that US27 promotes more CXCR4:IL-10R interactions.

CXCR4:IL-10R associations are highest in the presence of US27 with ligand binding

To quantify the impact of US27 on CXCR4:IL-10R interactions with ligand binding, we performed PLA on 293-US27 cells treated with CXCL12 or cmvIL-10 alone or in combination. Quantification of PLA spots showed that cells expressing US27 had

significantly more CXCR4:IL-10R associations than either HEK293 or 293-US28 cells, even in the absence of ligand binding (Fig 6A, light gray bars). While the addition of CXCL12 caused an increase in the number of CXCR4:IL-10R interactions in all three cell types (Fig 6A, dark gray bars), 293-US27 cells had the greatest number of PLA spots overall. Treatment with CXCL12 + cmvIL-10 also caused an increase in PLA spots in all three cell types (Fig 6A, black bars), with significantly more CXCR4:IL-10R interactions in cells expressing US27. The presence of US28 did not impact receptor clustering, and the number of CXCR4:IL-10R PLA spots was equivalent in HEK293 control and 293-US28 cells. These results suggest that US28 neither enhances nor impairs associations between CXCR4 and IL-10R. We also examined associations between US28 and CXCR4 during ligand binding. There were some detectable CXCR4:US28 punctae in untreated cells and an increase in puncta number occurred upon treatment with CXCL12 (Fig 6B). The number of CXCR4:US27 PLA spots was significantly higher than CXCR4:US28 PLA spots in untreated cells, and the number of CXCR4:US27 associations increased dramatically with CXCL12 treatment. Interestingly, the addition of cmvIL-10 to CXCL12 caused an even greater increase in CXCR4:US27 associations but did not impact associations between US28 and CXCR4. These findings demonstrate that CXCR4 specifically associates with IL-10R and US27.

CXCR4 associates with IL-10R and US27 during HCMV infection

Since we observed that CXCR4, IL-10R, and US27 are in close proximity in a 293-US27 cell line, we examined whether these receptors are also associated during virus infection when all of the other vGPCR (US28, UL33, UL78) were present. Newborn human foreskin fibroblasts (NuFF-1) were infected with BAC-derived HCMV laboratory strain AD169 expressing green fluorescent protein (GFP) (Yu et al., 2003). After 72 hours, the cells were fixed and PLA staining was performed. Both mock- and HCMV-infected NuFF-1 cells stained with antibodies against CXCR4 and IL-10R exhibited numerous red PLA spots, indicating that CXCR4:IL-10R associations also occur in fibroblasts and are not impaired by HCMV infection (Fig 7A). Staining with antibodies directed against IL-10R and the N-terminus of US27 resulted in numerous PLA spots in HCMV-infected cells. In direct contrast, very few PLA spots were detected in HCMV-infected cells stained with antibodies directed against IL-10R and the N-terminus of US28, suggesting that IL-10R preferentially associates with US27 and not US28, even when both are present. The observation that US28 does not associate with CXCR4 is consistent with previously published results (Frank et al., 2016; Tu et al., 2018). Staining with antibodies directed against CXCR4 combined with either US27-or US28-specific antibodies also indicated a specific and preferential association between US27 and CXCR4 (Fig 7B). Staining with two distinct CXCR4 antibodies served as positive control for detection of PLA spots during virus infection. Precise counting of the number of PLA spots per infected cell was not possible because morphological changes associated with CMV infection (Pooley et al., 1999; Resnik et al., 2000) made it difficult to delineate individual cells across images. Even without quantification, the number of PLA spots clearly indicates that both CXCR4 and IL-10R are found in close proximity with US27 during HCMV infection.

CXCR4 signaling is amplified during HCMV infection

Finally, we wanted to investigate the impact of US27 on CXCR4 signaling during virus infection in the presence of cmvIL-10. Since the calcium-sensitive dye Fluo-4 exhibits significant spectral overlap with GFP, we used HCMV strain TB40/E-*mCherry* (WT) or a mutant virus lacking US27 (US27Δ). NuFF-1 cells were infected at an MOI of 1 and after 72 hours labeled with Fluo-4 to measure fluorescence intensity as an indicator of intracellular calcium release. Mock infected cells released calcium in response to stimulation with CXCL12 (Fig 8, light gray bars), and the peak fluorescence intensity was higher when the stimulus was CXCL12 + cmvIL-10 (Fig 8, black bars), indicating more calcium mobilization. As expected, WT-infected cells exhibited the highest calcium flux when treated with CXCL12 + cmvIL-10 compared to mock and US27Δ infected cells. These results indicate US27 likely increases CXCR4:IL-10R interaction and confirm previous findings that US27 enhances CXCR4 signaling during virus infection (Tu et al., 2018). To confirm that enhanced CXCR4 signaling was specifically due to IL-10R ligands, we used two additional stimuli: interleukin-6 (IL-6) and Oncostatin M (OSM). When mock infected cells were treated with CXCL12 in combination with either IL-6 or OSM, the magnitude of the calcium response was the same as CXCL12 + PBS. The addition of PBS alone did not result in any calcium response. In WT and US27Δ cells, treatment with CXCL12 + IL-6 or OSM resulted in lower calcium levels than with CXCL12 + PBS, suggesting that other ligands may impair, rather than enhance, CXCL12-CXCR4 signaling responses. As a control, we treated cells with combinations of all the ligands (OSM + cmvIL-10, OSM + IL-6, IL-6 + cmvIL-10), but only treatments that included CXCL12 had induced significant calcium mobilization. There were no significant differences in levels of calcium flux between mock and US27Δ-infected cells for any ligand combination. Taken together, these results suggest that HCMV specifically enhances CXCL12-CXCR4 signaling during infection through cmvIL-10 and US27.

Conclusions

CXCR4 is an essential chemokine receptor that promotes cell growth, survival, and migration in response to CXCL12 binding. CXCR4 is also a tunable receptor whose signals can be dampened or amplified by interactions with other cellular receptors, and this is the first report of a specific association between CXCR4 and IL-10R. PLA results demonstrated that CXCR4 and IL-10R were within 30 nm of each other in multiple cell types and that ligand engagement enhanced CXCR4:IL-10R associations. HCMV infection increased the number of CXCR4:IL-10R PLA spots in fibroblasts, and this effect was attributable to the vGPCR, US27. Intriguingly, US28 did not impact CXCR4:IL-10R interactions, and neither US28 or the other vGPCR (UL33, UL78) interfered with the ability of US27 to associate with CXCR4 and IL-10R during HCMV infection. Because the correlation with receptor clustering and increased signal output was so clear, we did not investigate here whether the receptors were in direct contact or simply closely associated in membrane microdomains or lipid rafts, although this is potential area for future investigation. Our results clearly identify a novel signaling complex comprised of CXCR4, IL-10R, and US27 that dramatically enhances responses to CXCL12 during HCMV infection. The function of this complex during virus infection remains to be determined. As CXCL12 is highly expressed in stromal tissues and in the bone marrow (Moll and Ransohoff, 2010), we hypothesize that HCMV

amplifies chemotaxis of infected cells toward CXCL12 in order to facilitate virus persistence in stromal tissues. This is an extremely challenging hypothesis to test *in vivo* because murine CMV lacks homologs of either US27 or cmvIL-10. However, in a humanized mouse model of HCMV infection, CXCR4 antagonist AMD-3100 increased viral DNA in the liver (Smith et al., 2010), which was attributed to increased mobilization of latently infected myeloid lineage cells from the bone marrow. If blocking CXCL12-CXCR4 interactions leads to more virus infected cells in the periphery, then increasing migration of HCMV-infected cells into the bone marrow could also aid in infection of myeloid progenitors for the establishment or maintenance of latent reservoirs. In support of this notion, crosstalk of the CXCL12-CXCR4 and α4-integrin pathways mediates retention of neutrophils in the bone marrow (Petty et al., 2009). Additional studies are needed to understand the role of CXCR4 in HCMV infection.

Many viruses target the CXCL12/CXCR4 axis (Arnolds and Spencer, 2014). Human Immunodeficiency Virus (HIV) uses CXCR4 as a co-receptor for virus entry (Berson et al., 1996). Kaposi's sarcoma-associated herpesvirus (KSHV) blocks CXCR4 via cellular microRNAs (Punj et al., 2010) or the viral chemokine antagonist vMIP-II (viral macrophage inflammatory protein II) (Kledal et al., 1997) to promote release of infected cells into the bloodstream. Epstein-Barr virus (EBV) encodes a vGPCR, BILF1 that scavenges Gαi proteins to inhibit CXCL12/CXCR4 signaling (Nijmeijer et al., 2010). In contrast to EBV and KSHV, HCMV has several mechanisms to enhance CXCR4 expression and signaling (Arnolds et al., 2013; Boeck et al., 2018; Tu et al., 2018). While we have examined calcium flux and migration as signaling readouts, CXCL12 binding to CXCR4 activates several pathways, including NF-κB (Rehman and Wang, 2009; Teicher and Fricker, 2010), which promotes HCMV gene expression and replication (DeMeritt et al., 2004; DeMeritt et al., 2006; Kowalik et al., 1993; Sambucetti et al., 1989). The impact of CXCL12-CXCR4 signaling on HCMV gene expression and replication is currently unknown and requires further investigation.

To date we have focused on CXCR4 responses to CXCL12 signaling, but there are at least two other ligands for CXCR4: macrophage migration inhibitory factor (MIF) (Rajasekaran et al., 2016) and extracellular ubiquitin (Saini et al., 2010). HCMV infection induces MIF production (Bacher et al., 2002; Frascaroli et al., 2009), which could be a mechanism for keeping infected cells in peripheral tissues. Future studies are needed to study the impact of HCMV infection on MIF and ubiquitin signaling though CXCR4. Moreover, while we have observed that cmvIL-10 enhances CXCR4 downstream effects, we have not yet investigated the impact of CXCL12 on downstream signaling from the IL-10R, such as Stat3 activation or inhibition of inflammatory cytokines. It may be that crosstalk between the two receptors varies depending on the ligand, and additional work is needed to examine effects on IL-10R signaling due to hIL-10, cmvIL-10, or ebvIL-10 in the presence of CXCR4 agonists.

The successful co-existence of HCMV with its host requires extensive manipulation of host cellular processes. Our work demonstrates that CXCR4 is a prime target for manipulation during HCMV infection. Formation of a complex between CXCR4, IL-10R, and HCMV US27 could induce greater homing of infected cells to the bone marrow, releasing HCMV virions to expand the pool of latently infected progenitor cells. Furthermore, understanding

the novel virus-host receptor complexes that form during HCMV infection could aid in the quest for new and more effective anti-viral therapeutics.

Materials and Methods

Cells and Viruses

Human embryonic kidney cells (HEK293) (American Type Culture Collection, Manassas, VA) and newborn human foreskin fibroblasts (NuFF-1) (MTI-GlobalStem, Gaithersburg, MD) were cultivated in Eagles Minimal Essential Media (MEM) with 10% fetal bovine serum (FBS) (Atlanta Biologicals, Norcross, GA). HEK293 cells stably expressing HCMV US27 and US28 encoded in the p3X-FLAG vector (Sigma-Aldrich, St. Louis, Missouri) as described previously (Lares et al., 2013; Stapleton et al., 2012) were maintained in MEM supplemented with 10% FBS and 1 mg/ml Geneticin (Gibco, Grand Island, NY). All cells were cultivated at 37°C in a humidified incubator with an atmosphere of 5% CO_2. BAC-derived laboratory strain AD169-GFP (Yu et al., 2003) and BAC-derived clinical strains TB40/E-*mCherry* (WT) and TB40/EUS27Δ-*mCherry* (O'Connor and Shenk, 2011) virus stocks were used to infect confluent monolayers of NuFF-1 cells at a multiplicity of infection (MOI) of 1. Virus titers were determined using the $TCID_{50}$ method as described (O'Connor and Shenk, 2011).

Immunofluorescence microscopy

Cells were seeded onto FBS-coated glass coverslips in a 6-well plate at a density of 2×10^5 cells/well for 24 hours. The cell monolayer was washed once with Hanks's balanced salt solution (HBSS) with calcium and magnesium (Invitrogen, Grand Island, NY) and fixed with 4% paraformaldehyde for 20 minutes at room temperature (RT). Cells were washed and permeabilized with 0.2% (v/v) Triton-X-100 (Thermo Fisher, Waltham, MA) for 15 minutes at RT, then washed and blocked with HBSS + 10% bovine serum albumin (BSA) at 37°C for one hour. For colocalization studies, cells were co-stained with anti-CXCR4 goat polyclonal antibody (1:100, Santa Cruz) and anti-IL-10Rα rabbit polyclonal antibody (1:100, Santa Cruz) at 37°C for one hour, followed by FITC-conjugated donkey anti-goat secondary antibody and TRITC-conjugated goat anti-rabbit secondary antibody (Invitrogen) at 1:250 at 37°C for one hour. For four-color colocalization studies, cells were co-stained with anti-FLAG M2 mouse antibody (1:500, Sigma-Aldrich), anti-IL-10Rα rabbit polyclonal antibody (1:100, Santa Cruz), and anti-CXCR4 goat polyclonal antibody (1:100, Santa Cruz), followed by Alexa Fluor 514 goat-anti-mouse, Alexa Fluor 594 goat anti-rabbit, and Alexa Fluor 647 donkey anti-goat secondary antibodies (1:250, Invitrogen) at 37°C for one hour. Where indicated, cells were stained with anti-Oncostatin M receptor goat antibody (1:100, R&D Systems, Minneapolis, MN), followed by FITC-donkey anti-goat secondary antibody (1:250, Life Technologies, Carlsbad, CA). All coverslips were washed with HBSS and affixed to a slide with Prolong Gold mounting media with DAPI (Invitrogen). Specimens were imaged using a LSM700 laser scanning confocal microscope (Zeiss, Oberkochen, Germany) and Z-stack images are represented as maximum density projections.

Immunohistochemistry (IHC)

Paraffin-embedded tissue sections of human bone marrow (Zyagen, San Diego, CA) were immersed in xylene twice at 10 minutes each to remove paraffin, followed by a decreasing ethanol series: 100% ethanol, twice for 10 minutes followed by 95%, 70%, 50% ethanol, each for five minutes. Slides were rinsed with deionized water and rehydrated with PBS for 10 minutes followed by the addition of 10% BSA in phosphate-buffered saline (PBS) for 30 minutes at RT. After blocking, anti-CXCR4 goat polyclonal (1:100, Santa Cruz) and anti-IL-10Rα rabbit polyclonal antibody (1:100, Santa Cruz) were diluted in incubation buffer (1% BSA, 0.3% Triton X-100, and 0.01% sodium azide in PBS) and added onto slides with overnight incubation at 4°C. The next day, slides were washed in PBS three times for 15 minutes each followed by FITC-donkey anti-goat secondary antibody and TRITC-goat anti-rabbit secondary antibody (Invitrogen) each at 1:250 for one hour at RT. After secondary antibody incubation, slides were washed in PBS three times for 15 minutes. Coverslips with Prolong Gold were affixed and slides imaged as described above.

Proximity Ligation Assays

Cells were seeded into 16-well Lab-Tek chamber slides (Thermo Fisher Scientific, Waltham, MA) at 1×10^5 cells/well and then fixed with 4% paraformaldehyde for 10 minutes at RT. Slides were washed with PBS and permeabilized with 0.5% Triton X-100 in PBS. Where indicated, cells were co-stained with primary anti-CXCR4 goat polyclonal antibody (1:100, Santa Cruz), anti-IL-10Rα rabbit polyclonal antibody (1:100, Santa Cruz), anti-FLAG mouse monoclonal antibody (1:500, Sigma-Aldrich), anti-US27 (1:250, MAB203), anti-US28 mouse monoclonal antibody (1:100, Santa Cruz), anti-CXCR4 mouse polyclonal antibody (1:100, Santa Cruz) and/or Oncostatin-M receptor antibody (1:100, R&D Systems) at 37°C for one hour. The Duo Link *In Situ* Red Starter Kit (Sigma-Aldrich) was used and all washes and probe dilutions were carried out in accordance with the manufacturer's protocol, followed by Prolong Gold mounting medium. Specimens were imaged as above and quantification of punctae PLA spots was performed using Image J software.

Calcium Flux Assay

Calcium flux assay was performed as previously described (Tu et al., 2018). Briefly, a sample of 1×10^6 cells was resuspended in RPMI-1640 (Roswell Park Memorial Institute-1640) medium with no phenol red (Invitrogen, Grand Island, NY), 25 mM of HEPES (Invitrogen, Grand Island, NY) and labeled with Fluo-4AM (Invitrogen, Grand Island, NY) at a final concentration of 1 μM for 30 minutes, then washed and resuspended in fresh medium. Fluorescence intensity was measured for 20 seconds to establish baseline, then stimulus was added directly into the sample. Purified recombinant CXCL12 (Peprotech, Rocky Hill, NJ), cmvIL-10, Oncostatin-M, and IL-6 (R&D Systems) were used at 100 ng/ml. Sample data was collected using a BD Accuri C6 Flow Cytometer and analysis performed with FlowJo software.

Statistical Analysis

One way analysis of variance (ANOVA) was used to compare differences among different treatments group on the same cell type. The one tailed, type two Student's *t*-test was used

to determine statistical significance between treatments and controls or between the same treatment on different cell types.

Acknowledgements

We thank Jeff Oda at USF for excellent technical assistance. This work was supported by USF faculty development funds and NIH grant AI111232 (to JVS).

References

Arnolds KL, Lares AP, Spencer JV, 2013. The US27 gene product of human cytomegalovirus enhances signaling of host chemokine receptor CXCR4. Virology 439, 122–131. [PubMed: 23490053]

Arnolds KL, Spencer JV, 2014. CXCR4: a virus's best friend? Infect. Genet. Evol 25, 146–156. [PubMed: 24793563]

Arvin AM, Fast P, Myers M, Plotkin S, Rabinovich R, National Vaccine Advisory C, 2004. Vaccine development to prevent cytomegalovirus disease: report from the National Vaccine Advisory Committee. Clin. Infect. Dis 39, 233–239. [PubMed: 15307033]

Azevedo LS, Pierrotti LC, Abdala E, Costa SF, Strabelli TM, Campos SV, Ramos JF, Latif AZ, Litvinov N, Maluf NZ, Caiaffa Filho HH, Pannuti CS, Lopes MH, Santos VA, Linardi Cda C, Yasuda MA, Marques HH, 2015. Cytomegalovirus infection in transplant recipients. Clinics (Sao Paulo) 70, 515–523. [PubMed: 26222822]

Bacher M, Eickmann M, Schrader J, Gemsa D, Heiske A, 2002. Human cytomegalovirus-mediated induction of MIF in fibroblasts. Virology 299, 32–37. [PubMed: 12167338]

Balabanian K, Foussat A, Bouchet-Delbos L, Couderc J, Krzysiek R, Amara A, Baleux F, Portier A, Galanaud P, Emilie D, 2002. Interleukin-10 modulates the sensitivity of peritoneal B lymphocytes to chemokines with opposite effects on stromal cell-derived factor-1 and B-lymphocyte chemoattractant. Blood 99, 427–436. [PubMed: 11781221]

Beisser PS, Laurent L, Virelizier JL, Michelson S, 2001. Human cytomegalovirus chemokine receptor gene US28 is transcribed in latently infected THP-1 monocytes. J. Virol 75, 5949–5957. [PubMed: 11390596]

Berson JF, Long D, Doranz BJ, Rucker J, Jirik FR, Doms RW, 1996. A seven-transmembrane domain receptor involved in fusion and entry of T-cell-tropic human immunodeficiency virus type 1 strains. J. Virol 70, 6288–6295. [PubMed: 8709256]

Bodaghi B, Jones TR, Zipeto D, Vita C, Sun L, Laurent L, Arenzana-Seisdedos F, Virelizier JL, Michelson S, 1998. Chemokine sequestration by viral chemoreceptors as a novel viral escape strategy: withdrawal of chemokines from the environment of cytomegalovirus-infected cells. J. Exp. Med 188, 855–866. [PubMed: 9730887]

Boeck JM, Stowell GA, O'Connor CM, Spencer JV, 2018. The Human Cytomegalovirus US27 Gene Product Constitutively Activates Antioxidant Response Element-Mediated Transcription through Gbetagamma, Phosphoinositide 3-Kinase, and Nuclear Respiratory Factor 1. J. Virol 92, e00644–00618. [PubMed: 30209167]

Cannon MJ, 2009. Congenital cytomegalovirus (CMV) epidemiology and awareness. J Clin Virol 46 Suppl 4, S6–10.

Cannon MJ, Schmid DS, Hyde TB, 2010. Review of cytomegalovirus seroprevalence and demographic characteristics associated with infection. Rev. Med. Virol 20, 202–213. [PubMed: 20564615]

Casarosa P, Bakker RA, Verzijl D, Navis M, Timmerman H, Leurs R, Smit MJ, 2001. Constitutive signaling of the human cytomegalovirus-encoded chemokine receptor US28. J. Biol. Chem 276, 1133–1137. [PubMed: 11050102]

Casarosa P, Gruijthuijsen YK, Michel D, Beisser PS, Holl J, Fitzsimons CP, Verzijl D, Bruggeman CA, Mertens T, Leurs R, Vink C, Smit MJ, 2003. Constitutive signaling of the human cytomegalovirus-encoded receptor UL33 differs from that of its rat cytomegalovirus homolog R33 by promiscuous activation of G proteins of the Gq, Gi, and Gs classes. J. Biol. Chem 278, 50010–50023. [PubMed: 14522997]

Cheng S, Caviness K, Buehler J, Smithey M, Nikolich-Zugich J, Goodrum F, 2017. Transcriptome-wide characterization of human cytomegalovirus in natural infection and experimental latency. Proc. Natl. Acad. Sci. U. S. A 114, E10586–E10595. [PubMed: 29158406]

DeMeritt IB, Milford LE, Yurochko AD, 2004. Activation of the NF-kappaB pathway in human cytomegalovirus-infected cells is necessary for efficient transactivation of the major immediate-early promoter. J. Virol 78, 4498–4507. [PubMed: 15078930]

DeMeritt IB, Podduturi JP, Tilley AM, Nogalski MT, Yurochko AD, 2006. Prolonged activation of NF-kappaB by human cytomegalovirus promotes efficient viral replication and late gene expression. Virology 346, 15–31. [PubMed: 16303162]

Fraile-Ramos A, Kledal TN, Pelchen-Matthews A, Bowers K, Schwartz TW, Marsh M, 2001. The human cytomegalovirus US28 protein is located in endocytic vesicles and undergoes constitutive endocytosis and recycling. Mol. Biol. Cell 12, 1737–1749. [PubMed: 11408581]

Fraile-Ramos A, Pelchen-Matthews A, Kledal TN, Browne H, Schwartz TW, Marsh M, 2002. Localization of HCMV UL33 and US27 in endocytic compartments and viral membranes. Traffic 3, 218–232. [PubMed: 11886592]

Frank T, Reichel A, Larsen O, Stilp AC, Rosenkilde MM, Stamminger T, Ozawa T, Tschammer N, 2016. Attenuation of chemokine receptor function and surface expression as an immunomodulatory strategy employed by human cytomegalovirus is linked to vGPCR US28. Cell Commun Signal 14, 31. [PubMed: 27955674]

Frascaroli G, Varani S, Blankenhorn N, Pretsch R, Bacher M, Leng L, Bucala R, Landini MP, Mertens T, 2009. Human cytomegalovirus paralyzes macrophage motility through down-regulation of chemokine receptors, reorganization of the cytoskeleton, and release of macrophage migration inhibitory factor. J. Immunol 182, 477–488. [PubMed: 19109179]

Humby MS, O'Connor CM, 2015. Human Cytomegalovirus US28 Is Important for Latent Infection of Hematopoietic Progenitor Cells. J. Virol 90, 2959–2970. [PubMed: 26719258]

Jackson SE, Mason GM, Wills MR, 2011. Human cytomegalovirus immunity and immune evasion. Virus Res. 157, 151–160. [PubMed: 21056604]

Kledal TN, Rosenkilde MM, Coulin F, Simmons G, Johnsen AH, Alouani S, Power CA, Luttichau HR, Gerstoft J, Clapham PR, Clark-Lewis I, Wells TN, Schwartz TW, 1997. A broad-spectrum chemokine antagonist encoded by Kaposi's sarcoma-associated herpesvirus. Science 277, 1656–1659. [PubMed: 9287217]

Kotenko SV, Saccani S, Izotova LS, Mirochnitchenko OV, Pestka S, 2000. Human cytomegalovirus harbors its own unique IL-10 homolog (cmvIL-10). Proc. Natl. Acad. Sci. U. S. A 97, 1695–1700. [PubMed: 10677520]

Kowalik TF, Wing B, Haskill JS, Azizkhan JC, Baldwin AS Jr., Huang ES, 1993. Multiple mechanisms are implicated in the regulation of NF-kappa B activity during human cytomegalovirus infection. Proc. Natl. Acad. Sci. U. S. A 90, 1107–1111. [PubMed: 8381532]

Krishna BA, Miller WE, O'Connor CM, 2018. US28: HCMV's Swiss Army Knife. Viruses 10.

Lares AP, Tu CC, Spencer JV, 2013. The human cytomegalovirus US27 gene product enhances cell proliferation and alters cellular gene expression. Virus Res. 176, 312–320. [PubMed: 23850869]

Levoye A, Balabanian K, Baleux F, Bachelerie F, Lagane B, 2009. CXCR7 heterodimerizes with CXCR4 and regulates CXCL12-mediated G protein signaling. Blood 113, 6085–6093. [PubMed: 19380869]

Margulies BJ, Browne H, Gibson W, 1996. Identification of the human cytomegalovirus G protein-coupled receptor homologue encoded by UL33 in infected cells and enveloped virus particles. Virology 225, 111–125. [PubMed: 8918538]

Margulies BJ, Gibson W, 2007. The chemokine receptor homologue encoded by US27 of human cytomegalovirus is heavily glycosylated and is present in infected human foreskin fibroblasts and enveloped virus particles. Virus Res. 123, 57–71. [PubMed: 16963142]

Mocarski ES, Shenk T, Pass RF, 2006. Cytomegaloviruses. Lippincott-Raven Publishers, Philadelphia, PA.

Moll NM, Ransohoff RM, 2010. CXCL12 and CXCR4 in bone marrow physiology. Expert Rev. Hematol 3, 315–322. [PubMed: 21082982]

Nijmeijer S, Leurs R, Smit MJ, Vischer HF, 2010. The Epstein-Barr virus-encoded G protein-coupled receptor BILF1 hetero-oligomerizes with human CXCR4, scavenges Galphai proteins, and constitutively impairs CXCR4 functioning. J. Biol. Chem 285, 29632–29641. [PubMed: 20622011]

O'Connor CM, Shenk T, 2011. Human cytomegalovirus pUS27 G protein-coupled receptor homologue is required for efficient spread by the extracellular route but not for direct cell-to-cell spread. J. Virol 85, 3700–3707. [PubMed: 21307184]

Petty JM, Lenox CC, Weiss DJ, Poynter ME, Suratt BT, 2009. Crosstalk between CXCR4/stromal derived factor-1 and VLA-4/VCAM-1 pathways regulates neutrophil retention in the bone marrow. J. Immunol 182, 604–612. [PubMed: 19109194]

Pooley RJ Jr., Peterson L, Finn WG, Kroft SH, 1999. Cytomegalovirus-infected cells in routinely prepared peripheral blood films of immunosuppressed patients. Am J Clin Pathol 112, 108–112. [PubMed: 10396292]

Punj V, Matta H, Schamus S, Tamewitz A, Anyang B, Chaudhary PM, 2010. Kaposi's sarcoma-associated herpesvirus-encoded viral FLICE inhibitory protein (vFLIP) K13 suppresses CXCR4 expression by upregulating miR-146a. Oncogene 29, 1835–1844. [PubMed: 20023696]

Rajasekaran D, Groning S, Schmitz C, Zierow S, Drucker N, Bakou M, Kohl K, Mertens A, Lue H, Weber C, Xiao A, Luker G, Kapurniotu A, Lolis E, Bernhagen J, 2016. Macrophage Migration Inhibitory Factor-CXCR4 Receptor Interactions: EVIDENCE FOR PARTIAL ALLOSTERIC AGONISM IN COMPARISON WITH CXCL12 CHEMOKINE. J. Biol. Chem 291, 15881–15895. [PubMed: 27226569]

Rehman AO, Wang CY, 2009. CXCL12/SDF-1 alpha activates NF-kappaB and promotes oral cancer invasion through the Carma3/Bcl10/Malt1 complex. Int J Oral Sci 1, 105–118. [PubMed: 20695076]

Resnik KS, DiLeonardo M, Maillet M, 2000. Histopathologic findings in cutaneous cytomegalovirus infection. Am J Dermatopathol 22, 397–407. [PubMed: 11048974]

Saini V, Marchese A, Majetschak M, 2010. CXC chemokine receptor 4 is a cell surface receptor for extracellular ubiquitin. J. Biol. Chem 285, 15566–15576. [PubMed: 20228059]

Sambucetti LC, Cherrington JM, Wilkinson GW, Mocarski ES, 1989. NF-kappa B activation of the cytomegalovirus enhancer is mediated by a viral transactivator and by T cell stimulation. EMBO J. 8, 4251–4258. [PubMed: 2556267]

Sinclair J, 2008. Human cytomegalovirus: Latency and reactivation in the myeloid lineage. J. Clin. Virol 41, 180–185. [PubMed: 18164651]

Slobedman B, Barry PA, Spencer JV, Avdic S, Abendroth A, 2009. Virus-encoded homologs of cellular interleukin-10 and their control of host immune function. J. Virol 83, 9618–9629. [PubMed: 19640997]

Smith MS, Goldman DC, Bailey AS, Pfaffle DL, Kreklywich CN, Spencer DB, Othieno FA, Streblow DN, Garcia JV, Fleming WH, Nelson JA, 2010. Granulocyte-colony stimulating factor reactivates human cytomegalovirus in a latently infected humanized mouse model. Cell Host Microbe 8, 284–291. [PubMed: 20833379]

Soderberg-Naucler C, 2008. HCMV microinfections in inflammatory diseases and cancer. J. Clin. Virol 41, 218–223. [PubMed: 18164235]

Soderberg O, Gullberg M, Jarvius M, Ridderstrale K, Leuchowius KJ, Jarvius J, Wester K, Hydbring P, Bahram F, Larsson LG, Landegren U, 2006. Direct observation of individual endogenous protein complexes in situ by proximity ligation. Nat Methods 3, 995–1000. [PubMed: 17072308]

Sohy D, Parmentier M, Springael JY, 2007. Allosteric transinhibition by specific antagonists in CCR2/CXCR4 heterodimers. J. Biol. Chem 282, 30062–30069. [PubMed: 17715128]

Spencer JV, Lockridge KM, Barry PA, Lin G, Tsang M, Penfold ME, Schall TJ, 2002. Potent immunosuppressive activities of cytomegalovirus-encoded interleukin-10. J. Virol 76, 1285–1292. [PubMed: 11773404]

Stapleton LK, Arnolds KL, Lares AP, Devito TM, Spencer JV, 2012. Receptor chimeras demonstrate that the C-terminal domain of the human cytomegalovirus US27 gene product is necessary and sufficient for intracellular receptor localization. Virol J. 9, 42. [PubMed: 22339884]

Tadagaki K, Tudor D, Gbahou F, Tschische P, Waldhoer M, Bomsel M, Jockers R, Kamal M, 2012. Human cytomegalovirus-encoded UL33 and UL78 heteromerize with host CCR5 and CXCR4 impairing their HIV coreceptor activity. Blood 119, 4908–4918. [PubMed: 22496149]

Teicher BA, Fricker SP, 2010. CXCL12 (SDF-1)/CXCR4 pathway in cancer. Clin. Cancer Res 16, 2927–2931. [PubMed: 20484021]

Tu CC, Arnolds KL, O'Connor CM, Spencer JV, 2018. Human Cytomegalovirus UL111A and US27 Gene Products Enhance the CXCL12/CXCR4 Signaling Axis via Distinct Mechanisms. J. Virol 92.

Varnum SM, Streblow DN, Monroe ME, Smith P, Auberry KJ, Pasa-Tolic L, Wang D, Camp DG 2nd, Rodland K, Wiley S, Britt W, Shenk T, Smith RD, Nelson JA, 2004. Identification of proteins in human cytomegalovirus (HCMV) particles: the HCMV proteome. J. Virol 78, 10960–10966. [PubMed: 15452216]

Yu D, Silva MC, Shenk T, 2003. Functional map of human cytomegalovirus AD169 defined by global mutational analysis. Proc. Natl. Acad. Sci. U. S. A 100, 12396–12401. [PubMed: 14519856]

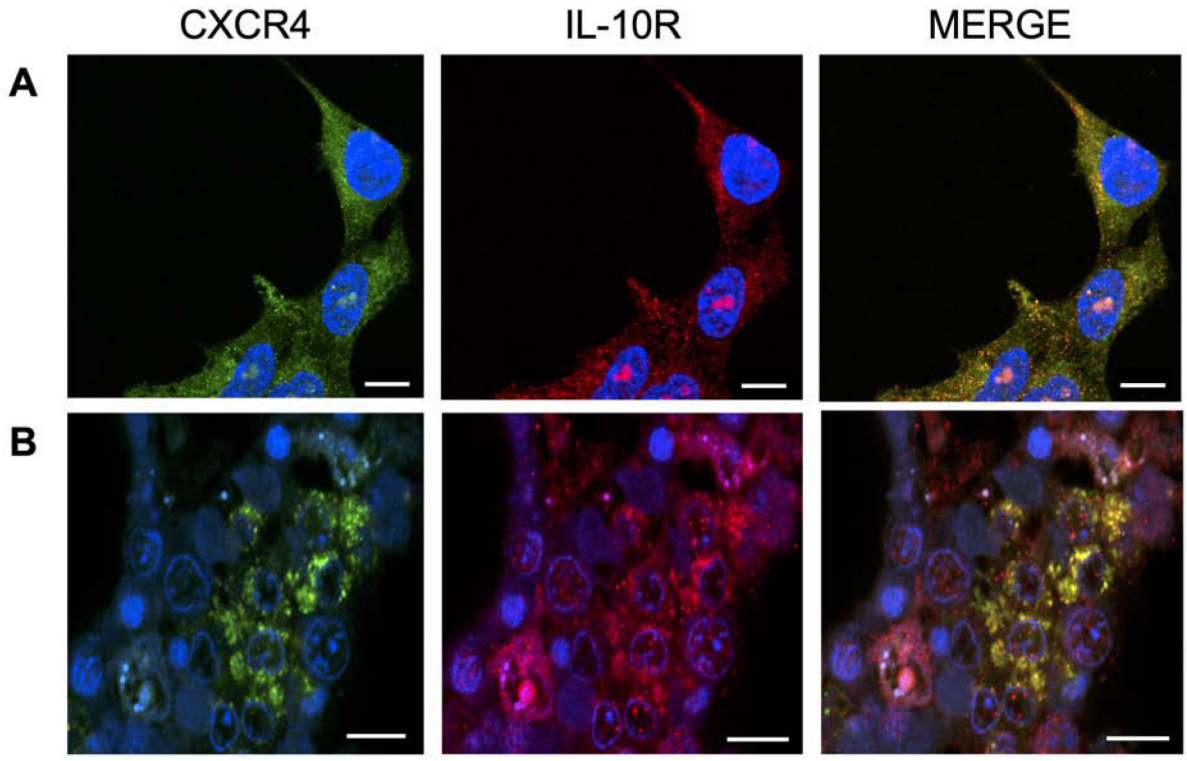

Figure 1. CXCR4 and IL-10R colocalize in cells in culture and in bone marrow.

A) HEK293 cells cultured on glass coverslips and stained with anti-CXCR4 goat antibody and anti-IL10R rabbit antibody followed by FITC-conjugated donkey anti-goat and TRITC-conjugated goat anti-rabbit secondary antibodies. Nuclei appear blue due to DAPI staining. B) Paraffin-embedded bone marrow tissue stained with the same antibodies as in A. Representative images are shown as maximum intensity projections from Z-stacks. Scale bar = 10 μm.

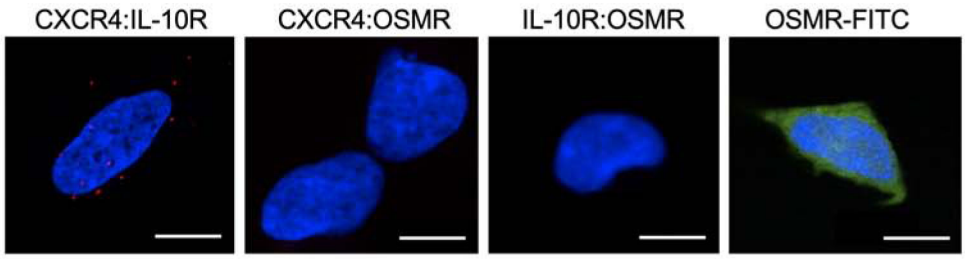

Figure 2. CXCR4 and IL-10R are in close proximity in human cells.

HEK293 cells cultured on glass coverslips were stained with primary antibodies to CXCR4, IL-10R, or OSMR in pairwise combinations as indicated, followed by secondary antibodies with oligonucleotide PLA+ or − probes. Red punctae indicate protein colocalization. The far right panel shows staining with anti-OSMR only followed by FITC-conjugated secondary antibody. Maximum intensity projection from Z-stack images taken by confocal microscopy. Scale bar = 10 μm.

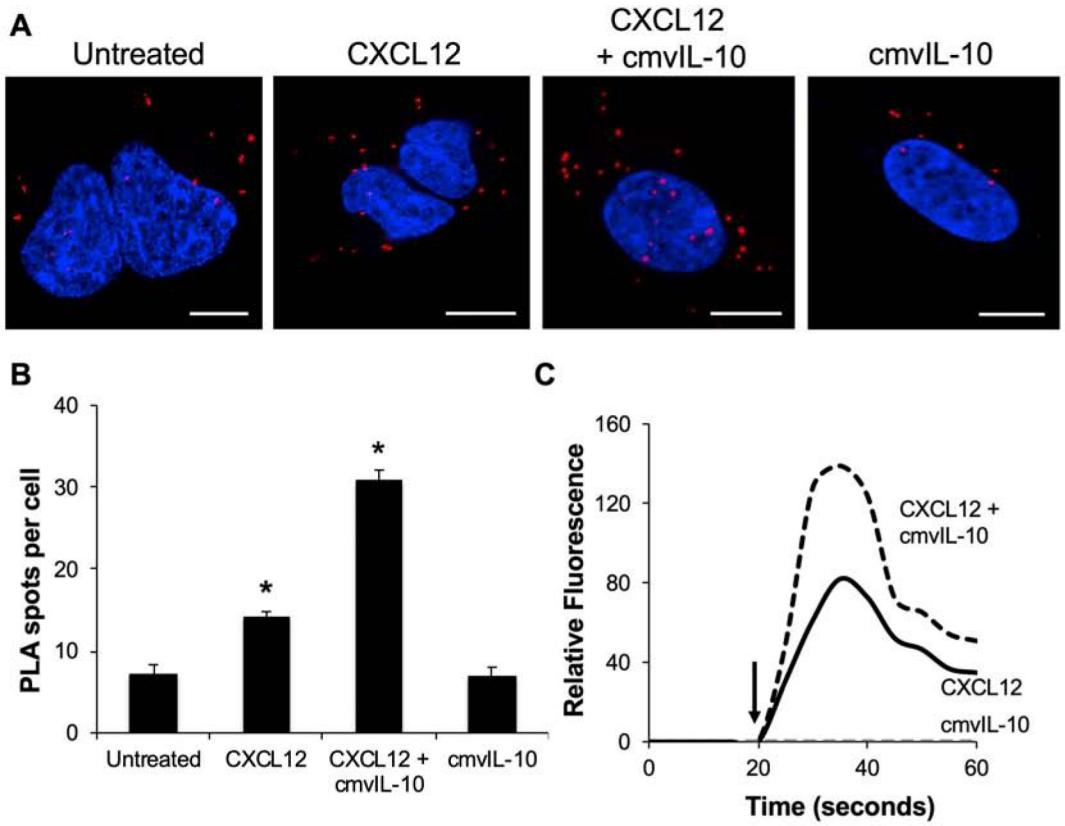

Figure 3. CXCR4 and IL-10R are in close proximity and cluster with ligand binding.

A) HEK293 cells cultured on glass coverslips were treated with 100 ng/ml chemokine or cytokine as indicated and stained with antibodies to CXCR4 and IL-10R followed by secondary antibodies with oligonucleotide PLA+ or − probes. Red punctae indicate protein colocalization. Maximum intensity projection from Z-stack images taken by confocal microscopy. Scale bar = 10 μm. B) Average number of spots per cell; 10 cells counted per treatment. Error bars, standard error of mean (SEM). *$p<0.00001$, paired Student's *t*-test vs. untreated, cmvIL-10, and each other. C) Calcium mobilization in HEK293 cells labeled with Fluo-4. Arrow indicates addition of 100 ng/ml stimulus: CXCL12 (solid black line), cmvIL-10 (gray dashed line), or CXCL12 + cmvIL-10 (black dashed line).

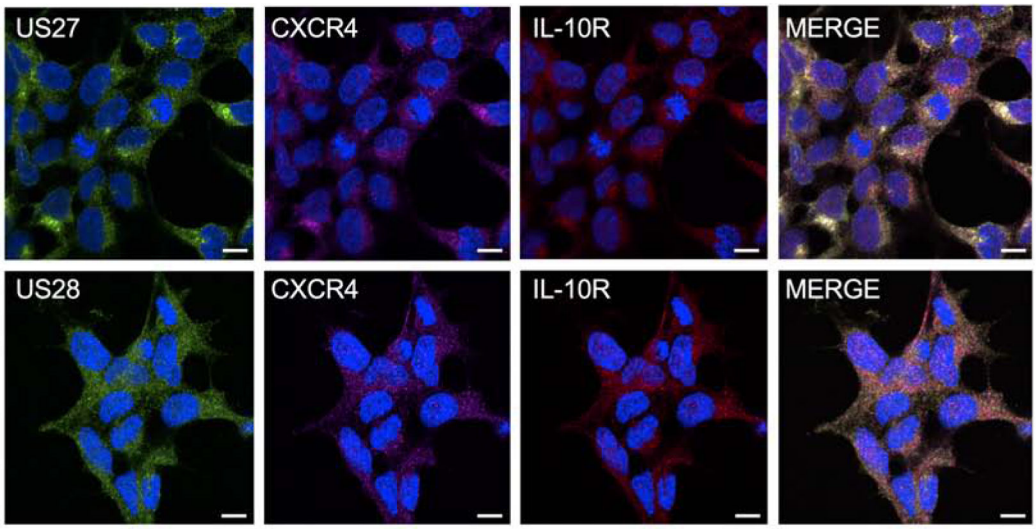

Figure 4. Colocalization of CXCR4, IL-10R, and HCMV US27.

HEK293 cells stably expressing US27 (top panel) or US28 (bottom panel) were grown on glass bottom chamber slides and co-stained with anti-FLAG mouse antibody, anti-CXCR4 goat polyclonal antibody, and anti-IL-10Rα rabbit polyclonal antibody, followed by Alexa Fluor 514 goat-anti-mouse secondary antibody, Alexa Fluor 647 donkey-anti-goat secondary antibody, and Alexa Fluor 594 goat-anti-rabbit secondary antibody, respectively. US27 or US28 (as indicated) is represented in green, CXCR4 in magenta, IL-10R in red, and areas of colocalization are represented in yellow in the merged images. Representative images are shown as maximum intensity projections from Z-stacks. Nuclei appear blue due to DAPI staining. Scale bar = 10 μm.

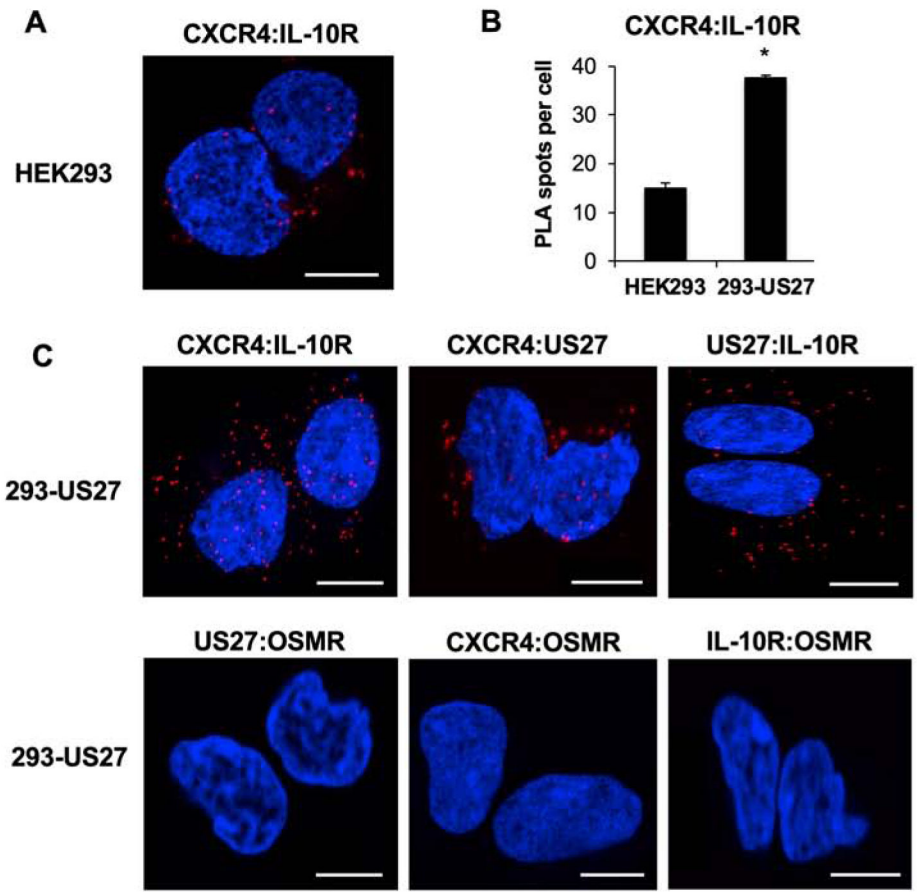

Figure 5. CXCR4 associates with IL-10R and HCMV US27.

A) HEK293 cells were grown in glass chamber slides and stained with primary antibodies against CXCR4 and IL-10R, followed by oligonucleotide-conjugated secondary antibodies for PLA. Maximum intensity projections from Z-stack images are shown. Nuclei appear blue due to DAPI staining. Scale bar = 10 μm. **B)** Quantification of discrete spots for CXCR4:IL-10R interactions, average of 10 cells. Error bars, SEM. *, $p < 0.001$ by paired Student's *t*-test. **C)** 293-US27 cells were grown in glass chamber slides and stained with primary antibodies against CXCR4, IL-10R, OSMR, and/or US27 followed by oligonucleotide-conjugated secondary antibodies for PLA as in A.

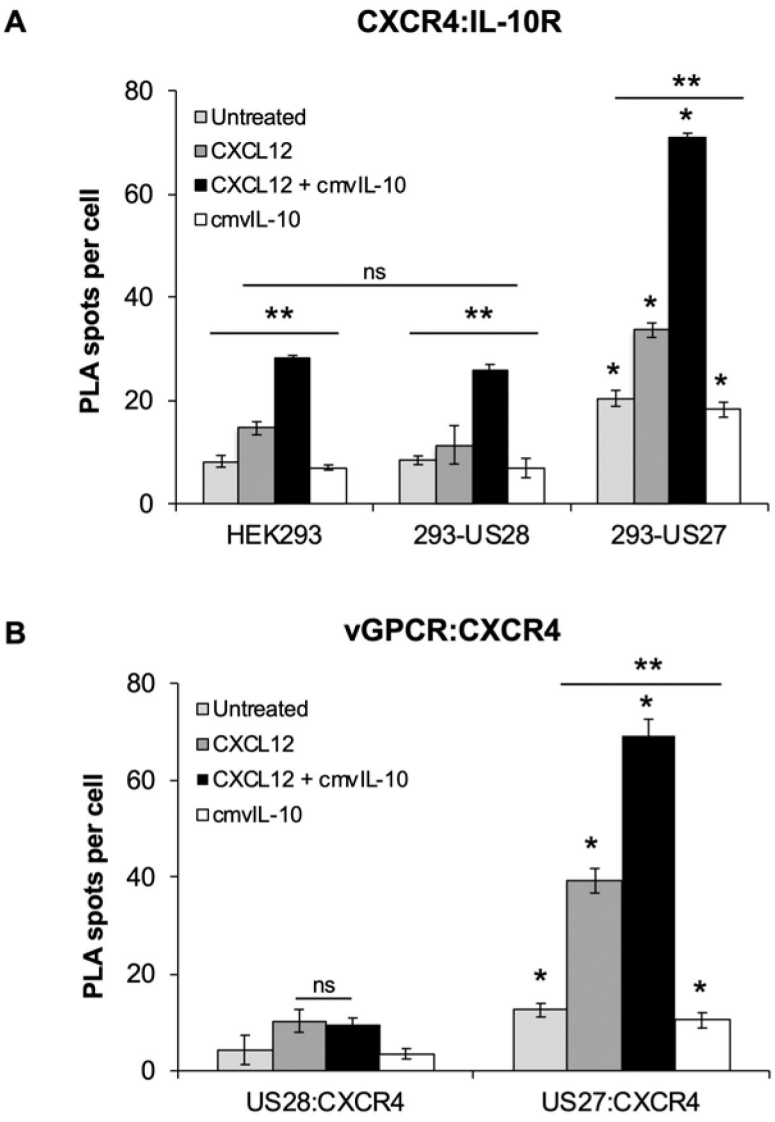

Figure 6. Ligand binding enhances CXCR4 clustering with other receptors.

A) Cells were treated with 100 ng/ml chemokine or cytokine as indicated then co-stained with primary anti-CXCR4 goat antibody and anti-IL10R rabbit antibody followed by PLA. **B)** 293-US27 or 293-US28 cells treated as above and co-stained with anti-FLAG mouse antibody and anti-CXCR4 goat antibody followed by PLA. For both panels, quantification from Image J was based on average of 10 cells. Error bars, standard error for 3 replicates; *p-value is <0.0001 by paired Student's *t*-test vs. corresponding treatment for HEK293 or 293-US28, ns = not significant by paired Student's *t*-test for corresponding treatments between HEK293 and 293-US28 or between treatments on 293-US28 cells as indicated. **p-value is < 0.00001 by one-way ANOVA for comparison of all treatments on the same cell type.

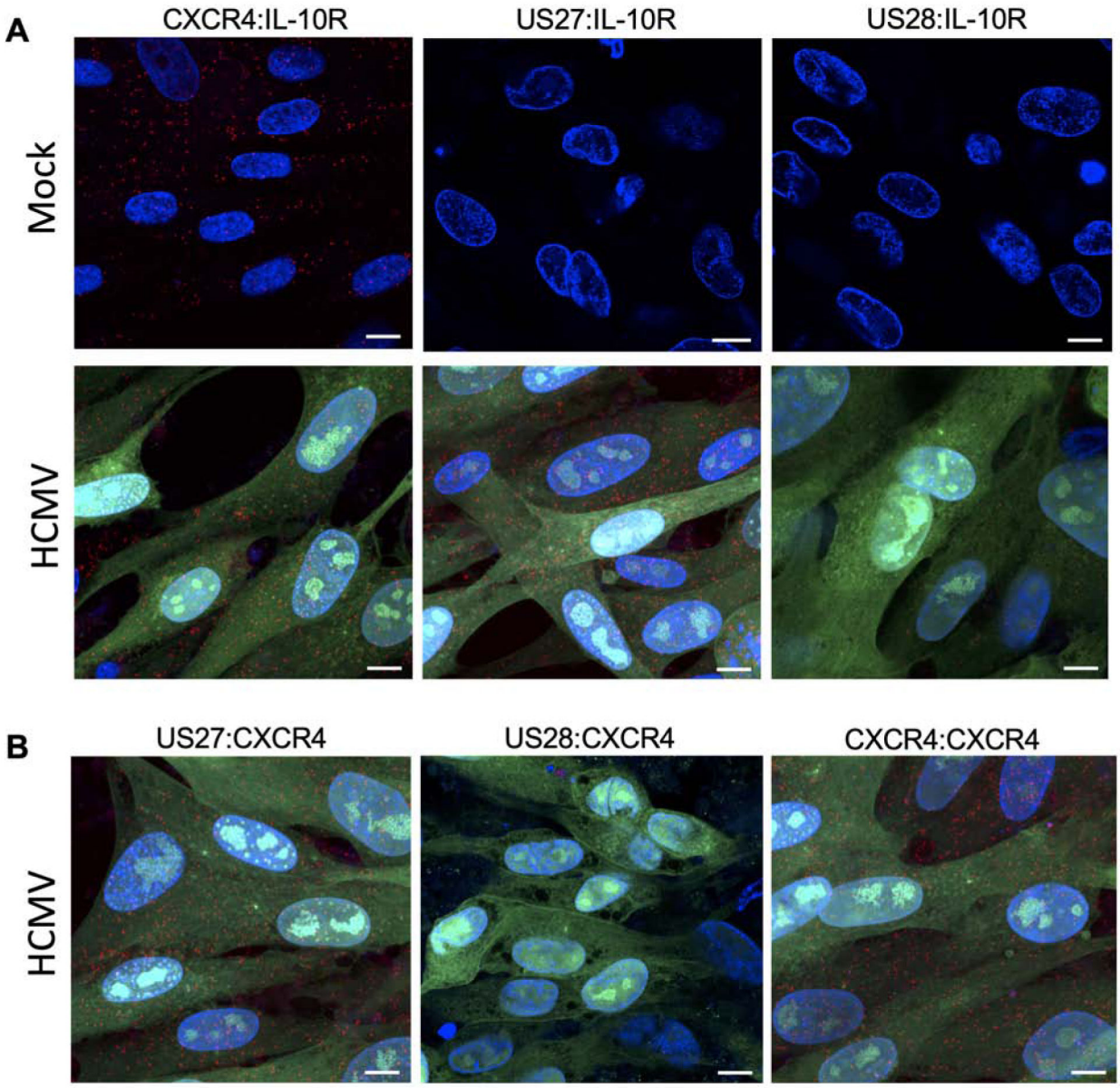

Figure 7. HCMV US27, CXCR4, and IL-10R associate during virus infection.

A) NuFF-1 cells were either mock infected or infected with HCMV AD169-GFP (MOI = 1, 72 hpi). Cells were stained with pairs of primary antibodies against CXCR4, IL10R, US27, or US28 as indicated followed by PLA. **B)** AD169-GFP infected NuFF-1 cells were stained with anti-CXCR4 (goat) and anti-US27, anti-US28, or anti-CXCR4 mouse as indicated followed by PLA. Nuclei appear blue due to DAPI staining. Representative images are shown as maximum intensity projections from Z-stacks. Scale bar = 10 μm.

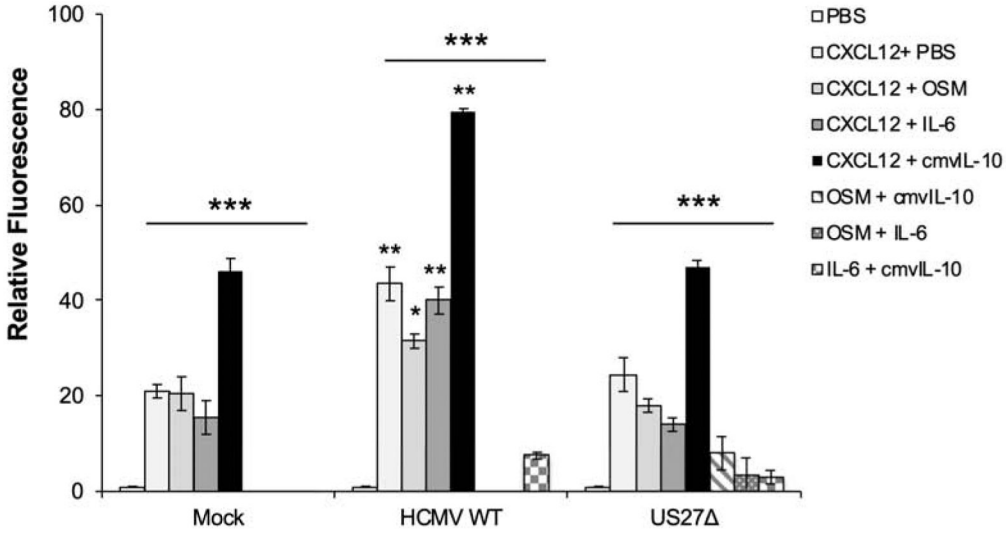

Figure 8. Specific ligand combinations increase calcium flux in HCMV infected cells.

NuFF-1 cells were infected with indicated virus and at 72 hpi, labeled with Fluo-4 and exposed to the indicated stimuli (100 ng/ml). Mean peak fluorescence intensity of duplicate samples is shown, and results are representative of three independent experiments. Error bar, standard error. *, $p < 0.05$ or **, $p < 0.005$ by paired Student's *t*-test vs. corresponding treatment on Mock or US27Δ-infected cells. ***$p < 0.0001$ by one-way ANOVA for comparison of all treatments on the same cell type.